CYBERNETICS AND PHYSICS, VOL. 13, NO. 3, 2024, 197–205

# INTERACTION OF TRAVELLING WAVES IN MULTILAYER NETWORKS

**Andrei V. Bukh**
Institute of Physics
Saratov State University
Russia
buh.andrey@yandex.ru

**Nataliya N. Nikishina**
Institute of Physics
Saratov State University
Russia
nnikishina7@gmail.com

**Eugene M. Elizarov**
Institute of Physics
Saratov State University
Russia
elizarovem5@gmail.com

**Galina I. Strelkova**
Institute of Physics
Saratov State University
Russia
strelkovagi@sgu.ru

Article history:
Received 14.10.2024, Accepted 12.11.2024

**Abstract**

In this paper, we explore numerically the impact of different types of inter-layer coupling on the dynamics of a two-layer multiplex network of coupled FitzHugh–Nagumo oscillators in the excitable regime. For this purpose, the cases of attractive, repulsive, and periodically modulated inter-layer coupling are considered. Coupled in the ring structure, the FitzHugh–Nagumo neurons demonstrate travelling wave regimes which are different for the attractive and repulsive intra-layer coupling. It is shown that the inter-layer coupling affects not only the frequency of oscillations of individual neurons but also the spatio-temporal structures in individual layers in different ways, depending on the sign of the inter-layer coupling. It is established that complete in-phase synchronization of travelling waves is well achieved in the presence of attractive inter-layer coupling, while the repulsive inter-layer coupling induces effective anti-phase synchronization of wave regimes. When the inter-layer coupling is periodically modulated, the wave structures in both layers are distorted, and clusters of coherent and incoherent dynamics can appear in the ring space. The paper was presented at PhysCon2024.

**Key words**

Travelling wave, FitzHugh–Nagumo neuron, multilayer network, attractive coupling, repulsive coupling

## 1 Introduction

Recently, the interaction of biologically relevant neurons has attracted particular attention of researchers in the connection with the development of the field of spiking neural networks [Yamazaki et al., 2022]. Spiking neural networks are functionally close to biological neural networks, since they implement temporal coding [Kasabov, 2019]. The most common biologically relevant neuron models are the Hodgkin–Huxley [Hodgkin and Huxley, 1952], Hindmarsh–Rose [Hindmarsh and Rose, 1984], Morris–Lecar [Morris and Lecar, 1981], Izhikevich [Izhikevich, 2003], and FitzHugh–Nagumo oscillators. The latter is the simplest and was proposed independently in [FitzHugh, 1961] and [Nagumo et al., 1962]. But even the simplest oscillatory FitzHugh–Nagumo neuron model is quite complicated, and attention should be paid to the dynamics of the individual neuron [Doi and Kumagai, 2005], including the influence of external signals [Yan et al., 2020], noise [Perc, 2005], and feedback with delay [Schöll et al., 2009], to the features of interaction of two coupled neurons with delay [Semenov et al., 2023] or coupled neurons that is induced by external noise [Hauschildt et al., 2006], and to the collective behavior of neurons in small [Rontogiannis and Provata, 2021] and large ensembles [Rybalova et al., 2021]. The authors of [Plotnikov, 2015] showed that a time-varying communication delay can influence the synchronization effect. In addition, optimal control of the collective behavior of the ensemble's neurons can be achieved through external influence [Takeuchi et al., 2012].

Networks of coupled FitzHugh–Nagumo neurons can demonstrate different spatio-temporal structures, such

as chimera states [Schöll, 2016] which are characterized by the coexistence of coherent and incoherent clusters [Abrams and Strogatz, 2004], and rotating waves [Perlikowski et al., 2010]. Inter-layer coupling between FitzHugh–Nagumo neuron networks can generate the competitive behavior between the solitary states and the chimeras in the transition to synchronous regime [Rybalova et al., 2021]. The authors of the paper [Sawicki et al., 2018] show that the delay controls chimera relay synchronization in multiplex neural networks. In addition, the influence of inter-layer coupling topology on the relay synchronization effect is investigated [Drauschke et al., 2020]. However, the issue of anti-phase synchronization arising due to repulsive inter-layer coupling has not been studied in sufficient detail. There are no practically data concerning the impact of inter-layer coupling of different types on traveling wave regimes in multiplex neural networks.

Basically, the coupling between FitzHugh–Nagumo neurons is electrical (gap junctions) or chemical [Li et al., 2007]. Besides, a generalized coupling in FitzHugh–Nagumo neuron networks was considered, including the links between activators, between inhibitors, and between activator and inhibitor variables [Omelchenko et al., 2013]. The electrical coupling between neurons can be attractive or repulsive, depending on the sign of the value of the coupling coefficient. The attractive coupling is general for biochemical systems, while the repulsive coupling occurs relatively rarely [Jiang et al., 2020]. For example, excitation-contraction coupling was employed in cardiac myocytes [Qu et al., 2007]. Repulsive coupling plays a crucial role in the dynamics of FitzHugh–Nagumo coupled neurons and significantly complicates the behavior of these neurons [Rybalova et al., 2023]. In this work, we investigate the influence of different types of inter-layer coupling on the spatio-temporal dynamics of two-layer multiplex neural networks. Depending on the intra-layer coupling, attractive or repulsive, uncopled layers initially demonstrate travelling waves of different form and different phase characteristics. The peculiarities of interaction of wave regimes are explored for attractive, repulsive and periodically modulated inter-layer coupling. The changes in the network dynamics as well as the possibilities of in-phase and anti-phase inter-layer synchronization are analyzed by using the mean frequency dependences and the Pearson's correlation coefficient.

## 2 Model under study

The object of our numerical simulation is a multiplex network of two coupled layers. Each layer represents a ring network of coupled FitzHugh–Nagumo neuron models proposed in [FitzHugh, 1961] and [Nagumo et al., 1962]. The multiplex network under study is described by the following system of equations:

$$\begin{aligned}\varepsilon\dot{x}_{i,k} &= x_{i,k} - \frac{x_{i,k}^3}{3} - y_{i,k} + \\ &+ \frac{\sigma_k}{2P}\sum_{j=i-P}^{i+P}(x_{j,k} - x_{i,k}) + \gamma_i(x_{i,l} - x_{i,k}), \\ \dot{y}_{i,k} &= x_{i,k} + a,\end{aligned} \tag{1}$$

where $x_{i,k}$ are the fast variables (activators) and represent the voltage across the cell membranes of neurons, $y_{i,k}$ are the slow recovery variables (inhibitors) which ensure that neurons return to the recovery state. The index $i = 1, 2, \dots N$ is the node number, and $N = 100$ is the total number of elements in each layer. The index $k, l = 1, 2, k \neq l$ are the layer numbers. The small parameter $\varepsilon$ is the ratio of the activator to inhibitor time scales. The parameter $a$ determines the excitation threshold in the single neuron. The FitzHugh–Nagumo oscillator can demonstrate either excitable ($|a| > 1$) or oscillatory ($|a| < 1$) regimes. In our study we set $\varepsilon = 0.01$, and $a = 1.05$ which corresponds to the excitable regime in each neuron.

The fourth term in the first equation of the network (1) is responsible for intra-layer coupling between neurons with the coupling strength $\sigma_k$ and the coupling range $P$. The links between neurons are electrical [Li et al., 2007]. The intra-layer coupling is attractive for the first layer and its coupling strength is set as a positive value $\sigma_1 = 0.1$. The repulsive intra-layer coupling is chosen for the second layer and its coupling strength is negative, $\sigma_2 = -0.1$.

The inter-layer coupling between the two layers is organized to be symmetrical and mutual. It is introduced via the $x$ variables and described by the last term in the first equation (1). In our simulation we consider three different cases of the inter-layer coupling strength distribution (Fig. 1). In the first case, the inter-layer coupling is attractive and flat, i.e., $\gamma_i = \gamma$ (green pluses and line in Fig. 1). In the second case, the coupling is repulsive and flat, i.e., $\gamma_i = -\gamma$ (red crosses and line in Fig. 1). And finally, a periodically modulated inter-layer coupling is used which is defined as $\gamma_i = \pi\gamma\sin(6\pi i/N)/2$ (black stars and line in Fig. 1). All the control parameters are dimensionless.

## 3 Quantitative measures

In order to analyze the "mean" behaviour of the coupled rings we calculate mean frequencies as follows:

$$\langle f_k \rangle = \frac{Q_k}{T \cdot N}, \tag{2}$$

where $Q_k$ is the number of spikes in the $k$th ring over time $T = 500$, $N$ is the number of neurons in the ring, $k = 1, 2$.

We also use Pearson's correlation coefficient $R_{1,2}$ [Pearson and Lee, 1903] between the $i$th neu-

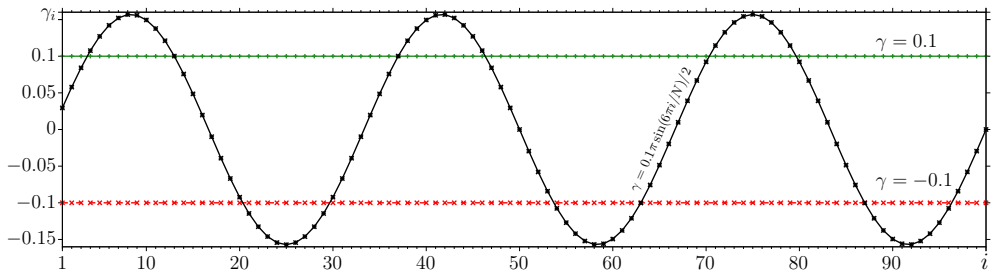


Figure 1. Methods of distributing the inter-layer coupling strength $\gamma_i$ for the cases of attractive links (green pluses and line), repulsive links (red crosses and line) and periodically modulated links (black stars and line) for same value of $\gamma = 0.1$ in the two-layer network (1)

rons of the coupled rings:

$$R_{1,2} = \frac{1}{N}\sum_{i=1}^{N}\Big(\Big(\sum_t (x_{i,1}(t) - \langle x_{i,1}\rangle_t)\times \\ \times (x_{i,2}(t) - \langle x_{i,2}\rangle_t)\Big)\Big/ \\ \Big/\Big(\sqrt{\sum_t (x_{i,1}(t) - \langle x_{i,1}\rangle_t)}\times \\ \times \sqrt{\sum_t (x_{i,2}(t) - \langle x_{i,2}\rangle_t)}\Big)\Big) \tag{3}$$

This measure gives evidence of the degree of correlation (synchronization) between the interacting layers. $R_{1,2}$ is varied within the interval $[-1, 1]$. The boundary values correspond to anti-phase and in-phase inter-layer synchronization of oscillations, respectively, and $R_{1,2} = 0$ relates to the case of a fully desynchronized multiplex network.

To evaluate the phase difference between the nodes in each layer and find its mean value we use the following relations:

$$\langle\varphi_i\rangle = \left\langle \sum_j \Delta\varphi_{j,j-1} \right\rangle_t, j = 1, 2, \ldots, i \\ \langle\varphi_i^{\text{even}}\rangle = \left\langle \sum_j \Delta\varphi_{j,j-2} \right\rangle_t, j = 2, 4, \ldots, i \tag{4} \\ \langle\varphi_i^{\text{odd}}\rangle = \left\langle \sum_j \Delta\varphi_{j,j-2} \right\rangle_t, j = 1, 3, \ldots, i,$$

where $\Delta\varphi_{j,j-1}$ is a phase difference between neurons $j, j-1$, and $\langle\cdot\rangle_t$ is the time average value. Other details of the behaviour are illustrated with additional plots.

## 4 Initial structures in uncoupled layers

When the layers are uncoupled, different kinds of travelling waves can be observed in the rings depending on the intra-layer coupling strength. The first layer demonstrates a wave pattern that is illustrated in Fig. 2,a–c. The corresponding space-time diagram $x_i(t) = x_{i,k}(t)$ and time series $x(t)$ for three selected neurons in the first layer are shown in Fig. 2,a, b, respectively. This regime is obtained for the positive intra-layer coupling strength $\sigma_1 = 0.1$ and represents a regular travelling wave with a small phase differences in the oscillations of neighboring neurons, which add up to $2\pi$ over a full traverse around the ring. The dependences $\langle\varphi_i\rangle, \langle\varphi_i^{\text{even}}\rangle, \langle\varphi_i^{\text{odd}}\rangle$ show similar results (see Fig. 2,c), and the mean frequency is $f_1 \approx 0.22$.

The second layer exhibits a distinct travelling wave regime which occurs due to the repulsive intra-layer coupling $\sigma_2 = -0.1$. Its characteristics is shown in Fig. 2,d–f. This kind of travelling waves differs from that in the first layer by a significant difference in the phases of oscillations of neighboring neurons (the black line in Fig. 2,f). In this case, the phases of oscillations of neurons with a difference in indices $i$ equal to 2 differ insignificantly and the sum of the phase difference along all even or odd neurons is equal to $2\pi$ (red and green lines in Fig. 2,h). Calculation of regular $\langle\varphi_i\rangle$ is not enough to detect the special travelling wave, and only $\langle\varphi_i^{\text{even}}\rangle, \langle\varphi_i^{\text{odd}}\rangle$ values can reveal it. The mean frequency of spikes of the nodes in the second layer is $f_2 \approx 0.21$.

## 5 Interaction of two travelling waves

We now explore the interaction of travelling waves in a two-layer network (1). The initial wave regimes are shown in Fig. 2,a, d. The impact of the inter-layer coupling is evaluated by calculating the mean frequency (2) for each layer and the correlation coefficient (3) between the coupled layers. The corresponding results are plotted in Fig. 3 for three different types of the inter-layer coupling, i.e., attractive flat with $\gamma_i = \gamma \geqslant 0$ (Fig. 3,a, d), repulsive flat with $\gamma_i = \gamma \leqslant 0$ (Fig. 3,b, e), and periodically modulated with $\gamma_i = \pi\gamma\sin(6\pi i/N)/2$ (Fig. 3,c, f). It should be noted that all frequency values $\langle f_k\rangle$ become equal for any $\gamma \neq 0, \gamma \in [-0.25, 0.25]$, although the initial frequency values in the uncoupled layers differ from each other.

In the case of attractive inter-layer coupling, the mean frequency $\langle f_k\rangle$ decreases linearly as the coupling strength $\gamma$ increases (Fig. 3,a). Herewith, the Pearson's correlation coefficient $R_{1,2}$ gradually increases as $\gamma \to$

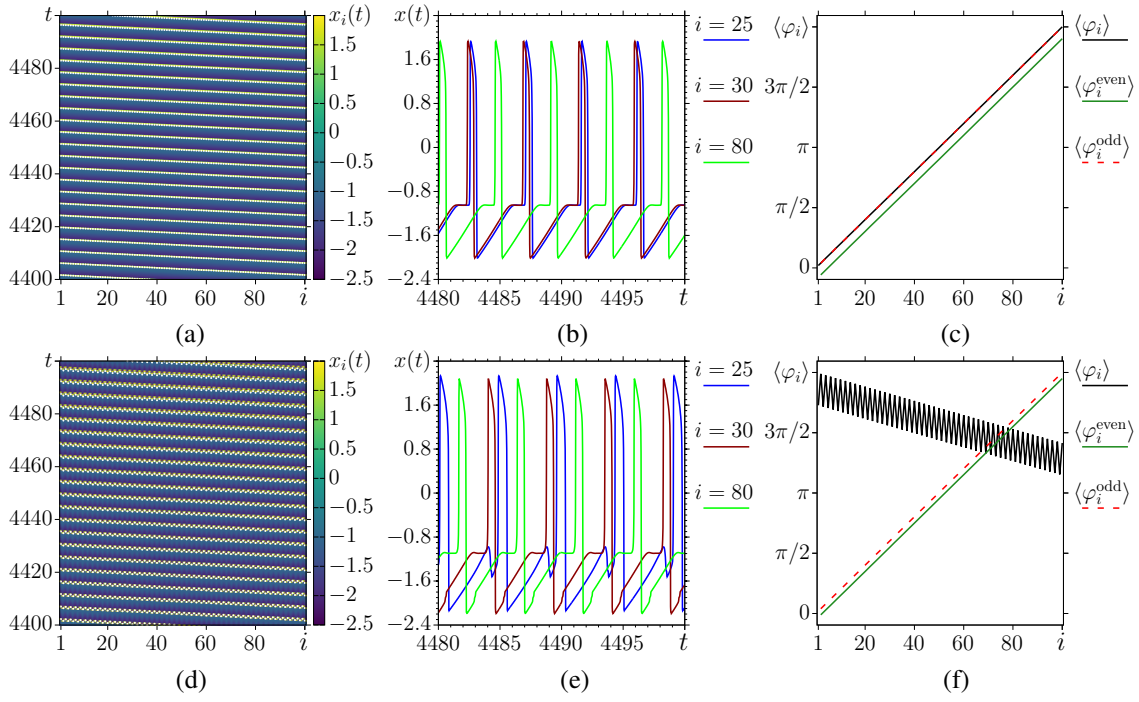


Figure 2. Initial wave structures in uncoupled layers ($\gamma_i = 0$ in (1)). Space-time diagrams $x_i(t) = x_{i,k}(t)$ (a, d), time series $x(t)$ for the chosen individual neurons (b, e), and phase differences $\langle\varphi_i\rangle$, $\langle\varphi_i^{\text{even}}\rangle$, $\langle\varphi_i^{\text{odd}}\rangle$ (c, f) for the first layer at $\sigma_1 = 0.1$ (a–c) and the second layer at $\sigma_2 = -0.1$ (d–f). Other parameters: $\varepsilon = 0.01, a = 1.05, P = 1, N = 100$.

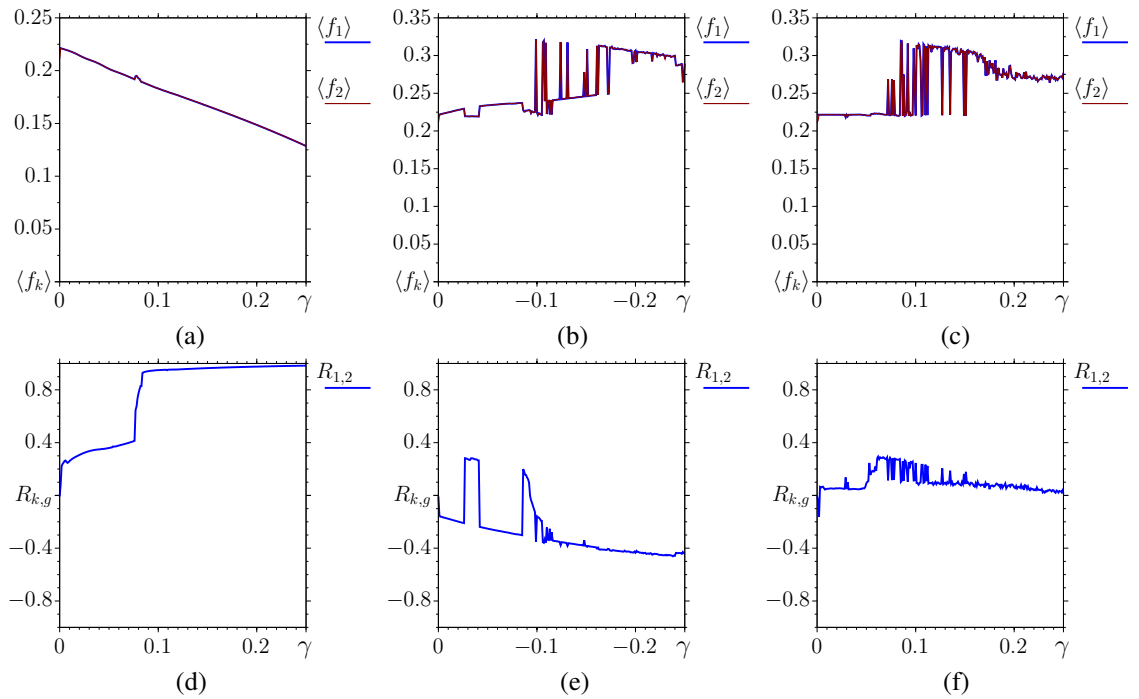


Figure 3. Mean frequencies $f_k$, $k = 1, 2$ (colors and line types are specified in legends) (a–c), and Pearson's correlation coefficient $R_{1,2}$ (d–f) for attractive flat inter-layer coupling $(\gamma \geqslant 0)$ (a, d), repulsive flat inter-layer coupling $(\gamma \leqslant 0)$ (b, e), and for periodically modulated inter-layer coupling ($\pi\gamma \sin(6\pi i/N)/2$) in the two-layer network (1). Other parameters: $\varepsilon = 0.01, a = 1.05, P = 1, N = 100$.

0.075 but remains less than 0.5 (Fig. 3,d). Thus, there is a range of the coupling strength $\gamma \in (0, 0.075]$ within which the frequencies become equal but the oscillations of the symmetrical nodes of the layers are still weakly correlated. This situation is illustrated in Fig. 4,a–c for

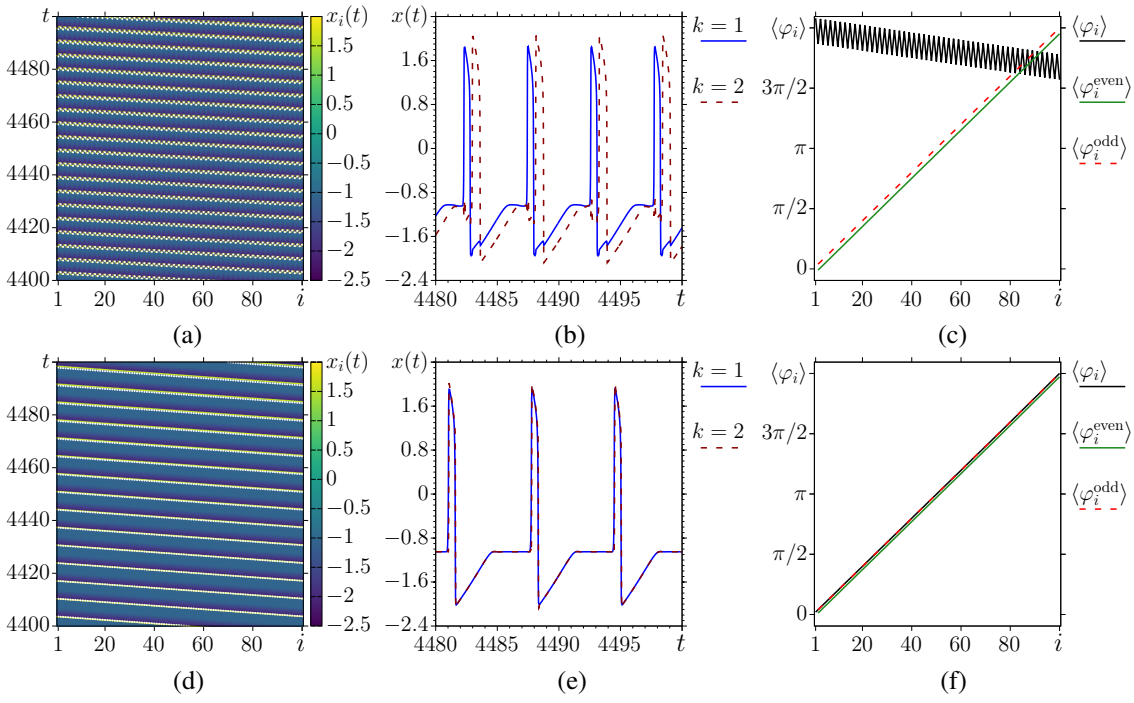


Figure 4. Space-time diagrams $x_i(t) = x_{i,2}(t)$ (a, d), time series $x(t)$ for the 50th node in each layer $k = 1, 2$ (b, e), and phase differences $\langle\varphi_i\rangle, \langle\varphi_i^{\text{even}}\rangle, \langle\varphi_i^{\text{odd}}\rangle$ (c, f) for the second layer ($k = 2$) for $\gamma = 0.07$ (a–c), and $\gamma = 0.2$ (d–f) in the two-layer network with attractive flat inter-layer coupling (1)). Other parameters: $\varepsilon = 0.01, a = 1.05, P = 1, N = 100$.

the fixed $\gamma = 0.07$ by the space-time diagram, time series for the 50th node of the layers, and phase differences (4) between the nodes in the second ring. It is clearly seen that for weak inter-layer coupling the travelling wave regime in the second ring doesn't change significantly.

Further increase in the inter-layer coupling, $\gamma > 0.075$, shows an abrupt increase in the correlation coefficient value $R_{1,2}$ which then tends to 1 with increasing $\gamma$ (Fig. 3,d). Starting with a certain value of attractive inter-layer coupling $\gamma \approx 0.15$ the layers become completely and in-phase synchronized. Exemplary spatio-temporal and phase characteristics of the synchronous regime established in both layers are presented in Fig. 4,d–f for $\gamma = 0.2$. It is seen that the interacting layers are synchronized in the regime of regular travelling wave being very similar to the initial wave structure in the first layer.

As follows from (Fig. 3,b,e), the dependence of the mean frequencies $\langle f_k\rangle$ on $\gamma$ looks like rather complicated in the case of repulsive inter-layer coupling (Fig. 3,b). However, a trend towards an increase in the oscillation frequencies can be observed when the coupling strength $\gamma$ decreases. Additionally, the Pearson's correlation coefficient $R_{1,2}$ takes negative values which decrease as $\gamma$ decreases (Fig. 3,e). Thus, one may conclude that the repulsive inter-layer coupling can induce an effect being quite similar to effective (within a finite accuracy) anti-phase inter-layer synchronization of wave structures in the two-layer multiplex network.

In order to explore the changes in the dynamics of coupled layers in details, we calculate and plots space-time diagrams and phase differences between the nodes in each layer in Fig. 5 for three different values of the repulsive inter-layer coupling strength. It can be seen that as a result of repulsive interaction, the initial travelling waves in the coupled rings can be distorted (the structure in the second layer, Fig. 5,a, g) or even destroyed (structures in both layers, Fig. 5,b, e, h). However, as the repulsive coupling strength increases in its absolute value, the travelling wave regime can be restored in both layers, and the observed wave structures almost exactly repeat the initial travelling waves (Fig. 2). Such a peculiarity of the multiplex network dynamics occurs when the repulsive inter-layer coupling strength is varied within the intervals $\gamma \in [-0.0159 : -0.0152] \cup [-0.0145 : -0.0132] \cup [-0.0129 : -0.0127] \cup [-0.0121 : -0.0115] \cup [-0.084 : -0.041] \cup [-0.026 : 0]$. However, the behavior of the second layer changes gradually as $\gamma$ decreases, and the travelling wave regime being very similar to the regular travelling wave can be established in the second layer (Fig. 5,c). However, there is a significant difference in the phases of oscillations of neighboring neurons (Fig. 5,i).

Now we turn to the third case when the inter-layer coupling is periodically modulated (black stars and line in Fig. 1). Calculation results for the mean frequencies and the correlation coefficient are shown in Fig. 3,c, f, respectively. In this case, it is impossible to detect a positive or negative trend in the dependence $\langle f_k\rangle(\gamma), k = 1, 2$ (Fig. 3,c). When the inter-layer coupling is weak,

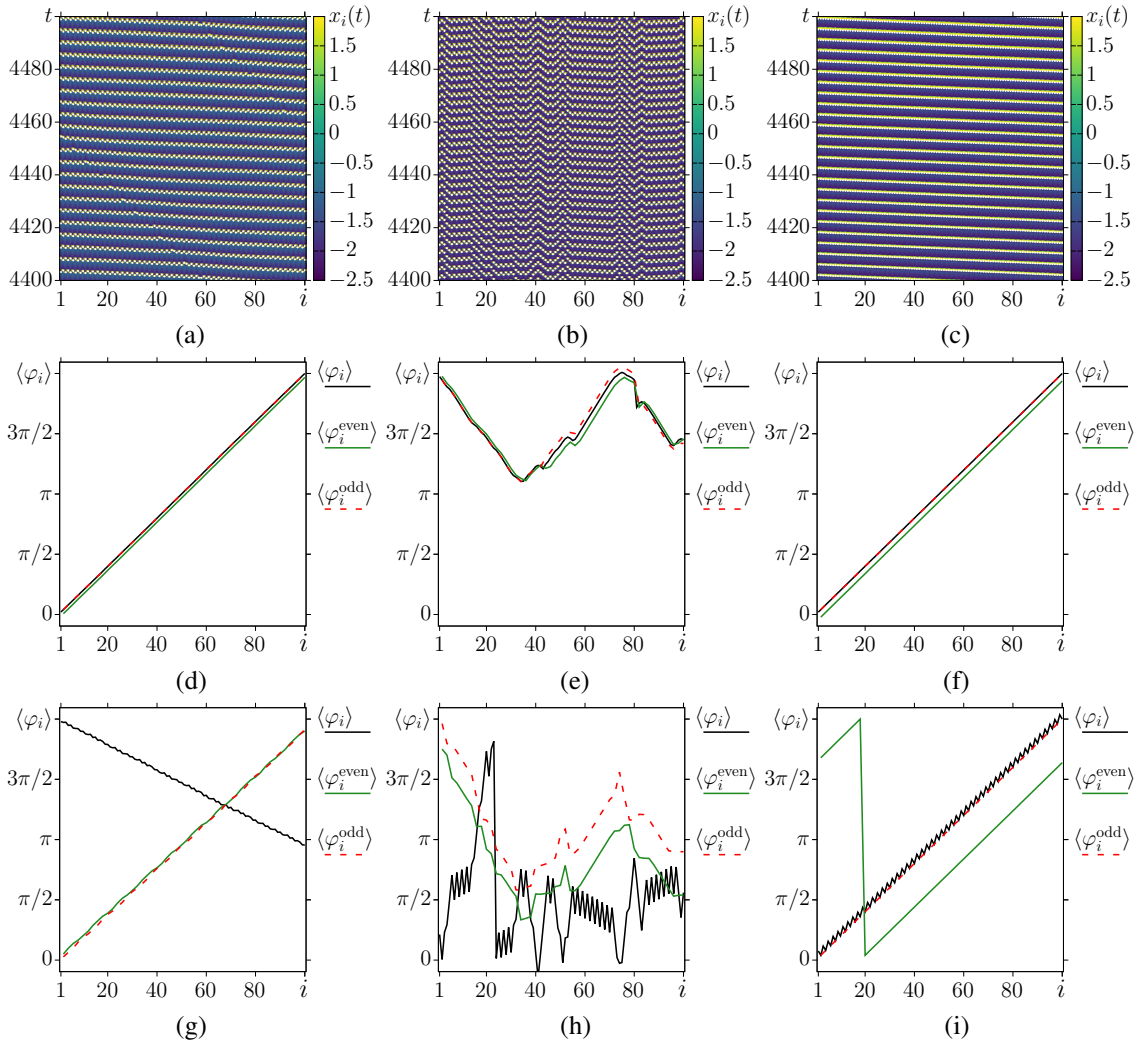


Figure 5. Space-time diagrams $x_i(t) = x_{i,2}(t)$ for the second layer ($k = 2$) (a–c) and phase differences $\langle\varphi_i\rangle$, $\langle\varphi_i^{\text{even}}\rangle$, $\langle\varphi_i^{\text{odd}}\rangle$ for the first layer (d–f) and the second layer (g–i) in the network (1) in the case of repulsive flat inter-layer coupling for $\gamma = -0.035$ (a, d, g), $\gamma = -0.099$ (b, e, h), and $\gamma = -0.155$ (c, f, i). Other parameters: $\varepsilon = 0.01, a = 1.05, P = 1, N = 100$.

$\gamma < 0.07$, and when the sum of all the inter-layer coupling strengths is equal to zero ($\sum_i \gamma_i = 0$), the mean frequency of neural impulses in the network remain unchanged and constant. Additionally, the Pearson's correlation coefficient $R_{1,2}$ is almost zero (Fig. 3,f). In this case, as follows from Fig. 6,a,d,g,j, where space-time diagrams and phase differences are shown for $\gamma = 0.04$ and for each layer separately, the regular travelling wave regime in the first layer has a more significant influence on the dynamics of the second layer in the case of weak periodically modulated inter-layer coupling. The same behavior of the multiplex network was also observed in the previous two cases (attractive flat and repulsive flat inter-layer couplings). The dynamical regime in the first layer is fully preserved (Fig. 6,a, g), while the wave structure in the second layer is distorted (Fig. 6,d, j).

When the coupling strength grows further, $\gamma \in [0.07, 0.152]$, the mean frequencies are arbitrarily changed between the constant level $f_1 \approx 0.22$ (as for weak coupling) and the frequency value from the range $f_1 \in [0.26, 0.35]$ (Fig. 3,c). The correlation coefficient $R_{1,2}$ changes arbitrarily its value between 0.1 and 0.3 (Fig. 3,f), that corresponds to weakly correlated oscillations of the interacting layers. A least correlated character ($R_{1,2} \to 0$) and thus the absence of synchronization between the two layers is also observed for larger values of inter-layer coupling, $\gamma > 0.15$ (Fig. 3,f). Such a picture can easily be understood if to address to the spatio-temporal and phase characteristics for each layer shown in Fig. 6,b, h, e, k for $\gamma = 0.081$ and Fig. 6,c, i, f, l for $\gamma = 0.2$. It is seen that several clusters of neurons appear in both layers (Fig. 6,b, e) but they are differently localized in the ring space. So, in the first layer, irregular (incoherent) clusters occupy the regions corresponding to repulsive inter-layer coupling with the second layer, while synchronous clusters in the second layer appear in places corresponding to attractive inter-layer coupling with the first layer. Thus, in the case of periodically mod-

ulated inter-layer coupling, the clusters of the spatio-temporal structure arising with attractive intra-layer coupling are transmitted by positive inter-layer coupling, and the clusters of the spatio-temporal structure resulted from the repulsive intra-layer coupling are transmitted by repulsive inter-layer coupling. Finally, when the periodically modulated inter-layer coupling becomes rather strong, $\gamma > 0.15$, the initial spatio-wave structures are essentially corrupted as can be seen in the corresponding space-time diagrams and phase differences for each layer (Fig. 6,c, i, f, l).

## 6 Conclusion

We have studied numerically how the type of inter-layer coupling, such as attractive, repulsive and periodically modulated, can influence the interaction of traveling waves in a two-layer network of coupled FitzHugh–Nagumo neurons. Without inter-layer coupling, the first layer with attractive intra-layer coupling demonstrates a regular travelling wave with a small phase difference in the oscillations of neighboring neurons, which adds up to $2\pi$ over a full traverse around the ring. The second layer also exhibits a travelling wave regime but due to the repulsive intra-layer coupling the phases of oscillations of neighboring neurons significantly differ, however, the sum of the phase difference along all even or odd neurons is equal to $2\pi$.

Our studies have shown that at weak attractive inter-layer coupling the mean frequencies of neuron impulses become equal but the oscillations of the symmetrical nodes remain weakly correlated. Starting with a certain value of the inter-layer coupling strength, the Pearson's correlation coefficient increases abruptly to 1, that indicates the effect of complete in-phase synchronization of traveling waves in the coupled layers.

In the case of repulsive inter-layer coupling, the dependence of the mean frequencies on the coupling strength becomes rather complicated, the Pearson's correlation coefficient takes negative values which decrease as the absolute value of the inter-layer coupling strength increases. The initial travelling waves in the coupled rings can be distorted or even destroyed. However, as the repulsive coupling strength increases in its absolute value, the travelling wave regime can be restored in each layers, and the observed wave structures almost exactly reproduce the initial travelling waves. It has been established that the repulsive inter-layer coupling has a significant effect on the dynamics of the multiplex neural network, changing the nature of the oscillations of the neurons in the layers, and can lead to the effect of anti-phase synchronization of traveling waves.

When the periodically modulated inter-layer coupling is weak enough, the mean frequency of neural impulses in the network remain unchanged and constant, and the Pearson's correlation coefficient is almost zero. When the coupling strength grows, the mean frequencies behave in a similar manner as in the case of repulsive coupling. The correlation coefficient first slightly increases and then again vanishes, thus indicating the uncorrelated dynamics between the layers. A new interesting fact has been revealed when studing the impact of periodically modulated inter-layer coupling. Several incoherent clusters appear in both layers and are characterized by a different length and location in the ring space. The clusters arising due to the attractive intra-layer coupling are transmitted by positive inter-layer coupling, and the clusters resulted from the repulsive intra-layer coupling are transmitted by repulsive inter-layer coupling. Finally, the initial spatio-wave structures in the layer are significantly distorted when the periodically modulated inter-layer coupling is sufficiently strong.

Thus, despite the complexity of the studied model and the coupling topology, it is possible to control the average frequency of oscillations in the network by introducing positive and negative links. The introduction of positive links leads to a decrease in the average frequency of oscillations, and the introduction of negative links, on the contrary, increases the average frequency of oscillations. The obtained results can be useful to specialists in the study and training of spiking neural networks. The initial distribution of links significantly affects the average frequency of spikes. Thus, if there is a need to introduce additional positive links between neurons for training purposes, negative links can also be introduced to maintain the average level of spike activity. Such an approach to training will allow avoiding a significant decrease or increase in the spike activity of network neurons on average.

As an outlook, it is worth exploring the behavioral features of a three-layer neural network and considering the possibilities of observing and controlling relay synchronization of traveling waves. Additionally, similar problems with non-identical parameters of excitability of neurons in the network are interesting. Distributed parameters of neurons will allow us to explore the permissible limits of observation of the effects presented in this article.

## Acknowledgements

The reported study was funded by the Russian Science Foundation (Project No. 20-12-00119). A.V.B. acknowledges the financial support provided by The Council for Grants of the President of the Russian Federation (Project No. SP-774.2022.5).

## References

Abrams, D. M. and Strogatz, S. H. (2004). Chimera states for coupled oscillators. *Physical review letters*, **93** (17), pp. 174102.

Doi, S. and Kumagai, S. (2005). Generation of very slow neuronal rhythms and chaos near the hopf bifurcation in single neuron models. *Journal of Computational Neuroscience*, **19**, pp. 325–356.

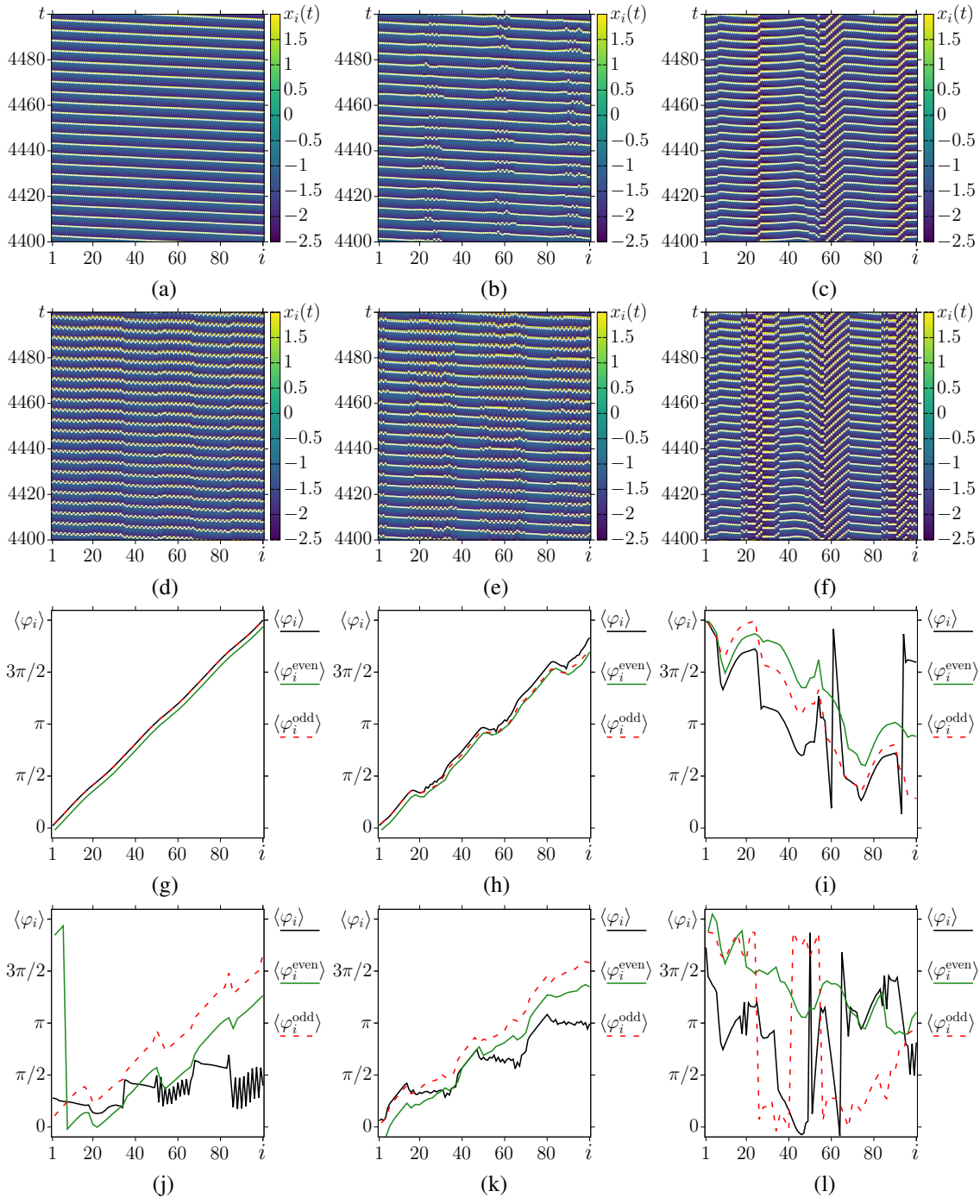


Figure 6. Space-time diagrams $x_i(t) = x_{i,1}(t)$ for the first layer (a–c) and $x_i(t) = x_{i,2}(t)$ for the second layer (d–f), and phase differences $\langle\varphi_i\rangle$, $\langle\varphi_i^{\text{even}}\rangle$, $\langle\varphi_i^{\text{odd}}\rangle$ for the first layer (g–i) and the second layer (j–l) in the case of periodically modulated inter-layer coupling for $\gamma = 0.04$ (a, d, g,j), $\gamma = 0.081$ (b, e, h, k), and $\gamma = 0.2$ (c, f, i, l). Other parameters: $\varepsilon = 0.01$, $a = 1.05$, $P = 1$, $N = 100$.

Drauschke, F., Sawicki, J., Berner, R., Omelchenko, I., and Schöll, E. (2020). Effect of topology upon relay synchronization in triplex neuronal networks. *Chaos: An Interdisciplinary Journal of Nonlinear Science*, **30** (5).

FitzHugh, R. (1961). Impulses and physiological states in theoretical models of nerve membrane. *Biophysical journal*, **1** (6), pp. 445–466.

Hauschildt, B., Janson, N., Balanov, A., and Schöll, E. (2006). Noise-induced cooperative dynamics and its control in coupled neuron models. *Physical Review E—Statistical, Nonlinear, and Soft Matter Physics*, **74** (5), pp. 051906.

Hindmarsh, J. L. and Rose, R. (1984). A model of neuronal bursting using three coupled first order differential equations. *Proceedings of the Royal society of Lon-*

*don. Series B. Biological sciences*, **221** (1222), pp. 87–102.

Hodgkin, A. L. and Huxley, A. F. (1952). A quantitative description of membrane current and its application to conduction and excitation in nerve. *The Journal of physiology*, **117** (4), pp. 500.

Izhikevich, E. M. (2003). Simple model of spiking neurons. *IEEE Transactions on neural networks*, **14** (6), pp. 1569–1572.

Jiang, Y., Wu, J., Yang, H., Xu, F., Wang, M., Huang, S., and Zhang, J. (2020). Chimera states mediated by nonlocally attractive-repulsive coupling in fitzhugh–nagumo neural networks. *Chinese Journal of Physics*, **66**, pp. 172–179.

Kasabov, N. K. (2019). *Time-space, spiking neural networks and brain-inspired artificial intelligence*. Springer.

Li, X., Wang, J., and Hu, W. (2007). Effects of chemical synapses on the enhancement of signal propagation in coupled neurons near the canard regime. *Physical Review E—Statistical, Nonlinear, and Soft Matter Physics*, **76** (4), pp. 041902.

Morris, C. and Lecar, H. (1981). Voltage oscillations in the barnacle giant muscle fiber. *Biophysical journal*, **35** (1), pp. 193–213.

Nagumo, J., Arimoto, S., and Yoshizawa, S. (1962). An active pulse transmission line simulating nerve axon. *Proceedings of the IRE*, **50** (10), pp. 2061–2070.

Omelchenko, I., Omel'chenko, O. E., Hövel, P., and Schöll, E. (2013). When nonlocal coupling between oscillators becomes stronger: Patched synchrony or multichimera states. *Physical review letters*, **110** (22), pp. 224101.

Pearson, K. and Lee, A. (1903). On the laws of inheritance in man: I. inheritance of physical characters. *Biometrika*, **2** (4), pp. 357–462.

Perc, M. (2005). Spatial coherence resonance in excitable media. *Physical Review E—Statistical, Nonlinear, and Soft Matter Physics*, **72** (1), pp. 016207.

Perlikowski, P., Yanchuk, S., Popovych, O., and Tass, P. (2010). Periodic patterns in a ring of delay-coupled oscillators. *Physical Review E—Statistical, Nonlinear, and Soft Matter Physics*, **82** (3), pp. 036208.

Plotnikov, S. (2015). Controlled synchronization in two fitzhugh-nagumo systems with slowly-varying delays. *Cybernetics and Physics*, **4** (1), pp. 21–25.

Qu, Z., Shiferaw, Y., and Weiss, J. N. (2007). Nonlinear dynamics of cardiac excitation-contraction coupling: an iterated map study. *Physical Review E—Statistical, Nonlinear, and Soft Matter Physics*, **75** (1), pp. 011927.

Rontogiannis, A. and Provata, A. (2021). Chimera states in fitzhugh–nagumo networks with reflecting connectivity. *The European Physical Journal B*, **94** (5), pp. 97.

Rybalova, E., Zakharova, A., and Strelkova, G. (2021). Interplay between solitary states and chimeras in multiplex neural networks. *Chaos, Solitons & Fractals*, **148**, pp. 111011.

Rybalova, E. V., Bogatenko, T. R., Bukh, A. V., and Vadivasova, T. E. (2023). The role of coupling, noise and harmonic impact in oscillatory activity of an excitable fitzhugh–nagumo oscillator network. *News of Saratov University. Ser. Physics*, **23** (4), pp. 294–306.

Sawicki, J., Omelchenko, I., Zakharova, A., and Schöll, E. (2018). Delay controls chimera relay synchronization in multiplex networks. *Physical Review E*, **98** (6), pp. 062224.

Schöll, E. (2016). Synchronization patterns and chimera states in complex networks: Interplay of topology and dynamics. *The European Physical Journal Special Topics*, **225**, pp. 891–919.

Schöll, E., Hiller, G., Hövel, P., and Dahlem, M. A. (2009). Time-delayed feedback in neurosystems. *Philosophical Transactions of the Royal Society A: Mathematical, Physical and Engineering Sciences*, **367** (1891), pp. 1079–1096.

Semenov, V. V., Bukh, A. V., and Semenova, N. (2023). Delay-induced self-oscillation excitation in the fitzhugh–nagumo model: Regular and chaotic dynamics. *Chaos, Solitons & Fractals*, **172**, pp. 113524.

Takeuchi, M., Konishi, K., and Hara, N. (2012). Optimal feedback control of traveling wave in a piecewise linear fitzhugh–nagumo model. *Cybernetics and Physics*, **1** (1), pp. 73–77.

Yamazaki, K., Vo-Ho, V.-K., Bulsara, D., and Le, N. (2022). Spiking neural networks and their applications: A review. *Brain Sciences*, **12** (7), pp. 863.

Yan, B., Panahi, S., He, S., and Jafari, S. (2020). Further dynamical analysis of modified fitzhugh–nagumo model under the electric field. *Nonlinear Dynamics*, **101**, pp. 521–529.